

Limits on the GeV Emission from Gamma-Ray Bursts

P. Beniamini ¹, D. Guetta ², E. Nakar ³ & T. Piran ⁴

¹ *Racah Institute of Physics, The Hebrew University, Jerusalem 91904, Israel; email: paz.beniamini@mail.huji.ac.il*

² *Osservatorio astronomico di Roma, v. Frascati 33, 00040 Monte Porzio Catone, Italy; email: dafne.guetta@oa-roma.inaf.it*

³ *Raymond and Beverly Sackler School of Physics & Astronomy, Tel Aviv University, Tel Aviv 69978, Israel; email: udini@wise.tau.ac.il*

⁴ *Racah Institute of Physics, The Hebrew University, Jerusalem 91904, Israel; email: tsvi@phys.huji.ac.il*

13 January 2013

ABSTRACT

The Large Area Telescope (LAT) on board of the Fermi satellite detected emission above 20 MeV only in a small fraction of the long gamma-ray bursts (GRBs) detected by the Fermi Gamma-ray Burst Monitor (GBM) at 8 keV - 40 MeV. Those bursts that were detected by the LAT were among the brightest GBM bursts. We examine a sample of the most luminous GBM bursts with no LAT detection and obtain upper limits on their high energy fluence. We find an average upper limit of LAT/GBM fluence ratio of 0.13 for GeV fluence during T_{90} and an average upper limit ratio of 0.45 for GeV fluence during the first 600 seconds after the trigger. These ratios strongly constrain various emission models and in particular rule out SSC models for the prompt emission. In about a third of both LAT detected and LAT non-detected bursts, we find that the extrapolation of the MeV range Band spectrum to the GeV range is larger than the observed GeV fluence (or its upper limit). While this excess is not highly significant for any specific burst, the overall excess in a large fraction of the bursts suggests a decline in the high energy spectral slope in at least some of these bursts. Possibly an evidence for the long sought after pair creation limit.

1 INTRODUCTION

GRBs were first discovered accidentally in the late sixties by the Vela satellite (Klebesadel et al. 1973). The Vela satellites detected photons at the 150-750 keV range. This led to several dedicated missions at the sub-MeV energy range. Indeed the peak of the energy flux was found to be in this energy range. For that reason, the main observational and theoretical efforts were made at this range. EGRET, the GeV detector on board the Compton Gamma Ray Observatory (CGRO), was

the first to detect GRBs at energies above 100 MeV (Schneid et al. 1992, Schneid et al. 1995). Two particular results of EGRET were extremely puzzling. The first, was a detection of an 18 GeV photon 1.5 hours after the burst in GRB 940217 (Hurley et al. 1994). The second, was the detection of a late time rising GeV spectral component in GRB 941017 (Gonzalez et al. 2003). For most of the bursts, though, there was no high energy (GeV) detection and only upper limits were obtained (Gonzalez Sanchez 2005) indicating that the GeV fluence is at most comparable to the MeV fluence (Ando et al. 2008).

At June 2008, NASA launched the Fermi gamma-ray space telescope which consists of two instruments. The LAT is a high energy (30 MeV to 300 GeV) detector. It has a larger energy range, a larger field-of-view (2.4 sr) and a shorter dead time (26 μ sec) than its predecessor EGRET (Atwood et al. 2009). The second instrument on board of Fermi, the GBM, covers the lower energy range of 8 keV to 40 MeV (Meegan et al. 2009), operating as a burst monitor. Up to February 2010, the LAT has detected 10 bursts at >100 MeV (LAT lookup table 2010) while at the same time the GBM detected over 400 bursts (GBM lookup table 2010). The LAT detected bursts continue to show those features first seen by EGRET. Namely, a delayed (Abdo et al. 2009a, Abdo et al. 2009b, Ackermann et al. 2010, Ghisellini et al. 2010) and prolonged (Abdo et al. 2009a) GeV emission as compared with the sub-MeV. The LAT fluence in all the LAT detected bursts was lower than, or comparable to, the GBM fluence (Ghisellini et al. 2010).

Understanding the properties of the GeV emission is crucial in order to answer two fundamental questions concerning GRBs: What is the emitting mechanism of the prompt gamma rays? and what is the origin of the high energy emission? For example, many authors (Mészáros et al. 1994, Waxman 1997, Wei & Lu 1998, Chiang & Dermer 1999, Panaitescu & Kumar 2000, Zhang & Mészáros 2001, Sari & Esin 2001, Guetta & Granot 2003, Fan & Piran 2008, Fan et al. 2008, Nakar et al. 2009, Dermer 2008, Finke & Dermer 2008) considered synchrotron Self Compton (SSC) as a mechanism for strong GeV emission. The ratio between the SSC Fluence and the synchrotron fluence is of order¹ $(\epsilon_e/\epsilon_B)^{1/2}$ (Sari et. al. 1996) (where ϵ_e is the fraction of energy in the electrons and ϵ_B is the fraction of energy in the magnetic field), and is therefore expected to be at least of order unity. Therefore limits on the GeV to MeV fluence, put strong limits on the SSC model and the conditions within the emitting region. SSC was also considered as a plausible radiation mechanism of the sub-MeV emissions (Panaitescu & Mészáros 2000, Kumar & McMahon

¹ Note that the Klein-Nishina limit plays no important role here, since upscattering of 100 keV photons to GeV is done in the Thomson regime by electrons with Lorentz factor of ~ 100 .

2008). Piran et al. (2009) have shown that this model is challenged by the lack of GeV emission that is brighter than the sub-MeV emission. Tighter limits on the GeV fluence will rule out this model entirely. Fan et al. (2009) has discussed the implications of a lack of strong GeV emission on the internal shocks model. He has shown that the model could work if there is a cutoff in the GeV due to pair creation and an SSC peak at the far TeV range. An alternative source of the GeV emission, motivated by the fact that it is prolonged, is that GeV emission arises from a different emitting zone than the prompt emission. This idea has been explored extensively in such models as the external shock afterglow model (Kumar & Barniol Duran 2009, Kumar & Barniol Duran 2010, Ghisellini et al. 2010, Piran & Nakar 2010, Gao et al. 2009, Granot & Guetta 2003, Corsi et al. 2010) and the multi-zone internal shocks model (Xue, Fan & Wei 2008, Aoi et al. 2009, Zhao, Li & Bai 2010).

The low LAT detection rate is consistent with a detection rate derived by assuming a ratio of 0.1 between the LAT and the GBM fluence and by extrapolating the MeV spectrum to the high energy range (Le & Dermer 2009). Although Guetta et al. (2011) find some GRBs that by extrapolating their MeV fluence to the GeV window should have been detected by LAT, but were not. Therefore, putting upper limits on the fluence ratio is crucial in order to test the nature of the spectrum at high energies. This, in turn, will further constrain the emitting mechanism. For example, in the case of pure synchrotron, we might expect an extrapolation of the sub-MeV spectrum, while for SSC we might see a rising spectral slope in the sub-GeV. There has been one example of such a rising spectral slope in the famous GRB 090902B (Abdo et al. 2009b), but the overall picture is still highly uncertain.

In an earlier study, Guetta et al. (2011) have used the non-detection of GeV emission from the majority of Fermi GRBs, to put upper limits on the GeV fluence of long GRBs. They find an upper limit on the LAT/GBM fluence ratio of less than unity for 60% of GRBs. This is consistent but not better than the EGRET-derived limits (Ando et al. 2008). In this paper, we use a more subtle approach to further constrain these limits. As the LAT detected GRBs are also among the brightest GRBs in the GBM band (Swenson et al. 2010), we examine the brightest group of GBM bursts with no LAT detection. Those are expected to be the bursts with the highest undetected GeV fluence. We obtain upper limits on their GeV fluence and use them to gain more stringent upper limits on the LAT/GBM fluence ratio. As the LAT emission is extended we obtain limits for both the duration of the prompt MeV emission, T_{90} , and for the extended duration of 600 sec. These limits rule out SSC as a model for the prompt emission, and put further constraints on many proposed emission mechanisms.

2 THE SAMPLE

We consider all long ($T_{90} \geq 2$ seconds) GRBs detected by GBM by February 2010. The GBM has a much wider ($\sim 8\text{sr}$) field of view than the LAT ($\sim 2.4\text{sr}$). After the GBM detects a bright enough GRB, according to some selection criteria, Fermi slews the LAT bore-sight towards the GBM position. We consider only GBM-detected bursts within the LAT field of view. To minimize the effect of slewing (towards the burst or due to the regular motion of the spacecraft) we consider only bursts with small bore-sight angles. It should be stressed that in the following analysis, we do not try to mimic the complicated slewing behaviour of the burst, but rather we develop a method which largely overcomes the difficulties posed by this slewing. As mentioned in §1, those GRBs with a LAT detection, are the brightest GRBs in the GBM range. Therefore we expect the brightest GBM bursts with no GeV detection to be the brightest GeV bursts undetected by LAT. These are also the bursts for which we can obtain the tightest limits on the sub-MeV to GeV fluence ratio.

Taking the above considerations into account, our sample of bursts detected only by the GBM (denoted as the "GBM sample") includes the 18 most fluent long GRBs (within the LAT viewing angle and with a bore-sight angle of less than 60° ²) that were detected by the GBM and undetected by LAT. This corresponds to bursts with GBM fluence over $8.3 \times 10^{-6} \text{ erg/cm}^2$. The seemingly random choice of lower limit on the fluence is taken from the number of bursts we consider. If we were to find any significant GeV signal, it would have made sense to change this limit in accordance and look at additional bursts, but this was not the case. For all bursts in the sample, we take all the $>100\text{MeV}$ photons (as seen by the LAT) whose positions in the sky are up to 15° from the GBM position. The GBM position error is $\sim 10^\circ$ and can be even less for bright bursts (Briggs et al. 2009). Therefore, the source of the LAT fluence (if such a source exists) is very likely within the data set.³ We only take photons with a bore-sight angle of less than 60° as the LAT effective area per photon decreases rapidly for viewing angles larger than 60° .

We also consider a sample of LAT detected bursts (denoted the "LAT sample") that consists of the 10 bursts with a reported detection by the LAT team during the same period. A GRB is tagged as detected by the LAT if the number of photons detected, N_s , exceeds 10 and if it exceeds a 5σ fluctuation of the background (Band et al. 2009, Atwood et al. 2009). These bursts include: 080916C, 080825C, 090217, 090323, 090328, 090626, 090902B, 090926A, 091003A, 091031.

² The effective area decreases rapidly for larger bore-sight angles. This selection criteria reduces the errors in the fluence due to the varying bore-sight angle.

³ As a check to this statement, we found that we obtain similar results when taking photons from up to 10° from the GBM position only

Note that so far the LAT team published detailed fluence measurements only for four of those bursts: 080825C, 080916C, 090217, 090902B (Abdo et al. 2010).

3 THE MODEL - OVERVIEW

Our goal is to obtain an upper limit on the GeV fluence of each of the bursts in the GBM sample. A complete approach involves maximizing a general likelihood function, for which the free parameters are: the burst's position, (x,y) , the ratio, r , between the burst's fluence and the total (burst+noise) fluence, and the spectral parameters of both the burst $N \sim E^{-\alpha}$ and the noise $N_{noise} \sim E^{-\beta}$. The likelihood function is:

$$L'(x, y, r, \alpha, \beta) = \prod_{i=1} A(E_i, \theta_i) P(x, y, x_i, y_i, E_i) [rN(E_i) + (1-r)N_{noise}(E_i)] , \quad (1)$$

where the summation is over all photons within 15° of the GBM position from $t=0$ to $t=T$ (T can be T_{90} or 600 sec depending on the assumption on the origin of the GeV emission). x_i, y_i are the right ascension and declination of the i 'th photon in local Cartesian coordinates.⁴ $P(x, y, x_i, y_i, E_i)$ is the probability that a photon with energy E_i from a burst at (x,y) will be detected at (x_i, y_i) , namely it is the value of the LAT point spread function for photon energy E_i at the angle between (x,y) and (x_i, y_i) (Atwood et al. 2009).

Unfortunately, this method turns out to depend strongly on the unknown spectrum of the noise N_{noise} , and it cannot be used. We turn to a different approach which is more stable. We split the process into two phases. First we find the most probable positions of the bursts using a simpler likelihood procedure. Then, using these positions we calculate fluence upper limits.

3.1 Bursts' positions

We find the most probable position of a burst by maximizing the likelihood, L , that it is located at (x,y) :

$$L(x, y) = \prod_{i=1} A(E_i, \theta_i) N(E_i) P(x, y, x_i, y_i, E_i) . \quad (2)$$

Fig. 1 depicts an example of this likelihood function for burst 081231. To calculate the likelihood function we need the burst's spectrum, $N(E)$. We assume $N \propto E^{-2}$. We allow for variation in the slope of the spectrum and find that the dependence of the position on this parameter is weak.

⁴ The plane of right ascension and declination (in which the photons locations are given) is not a flat plane but a surface of a sphere. As we are only dealing with locations within 15° from the GBM location, we can (to a very good approximation) use a locally flat coordinate system. This is done by taking the projection of each position on the sphere to the plane tangent to the sphere at the GBM position. These are the x,y coordinates.

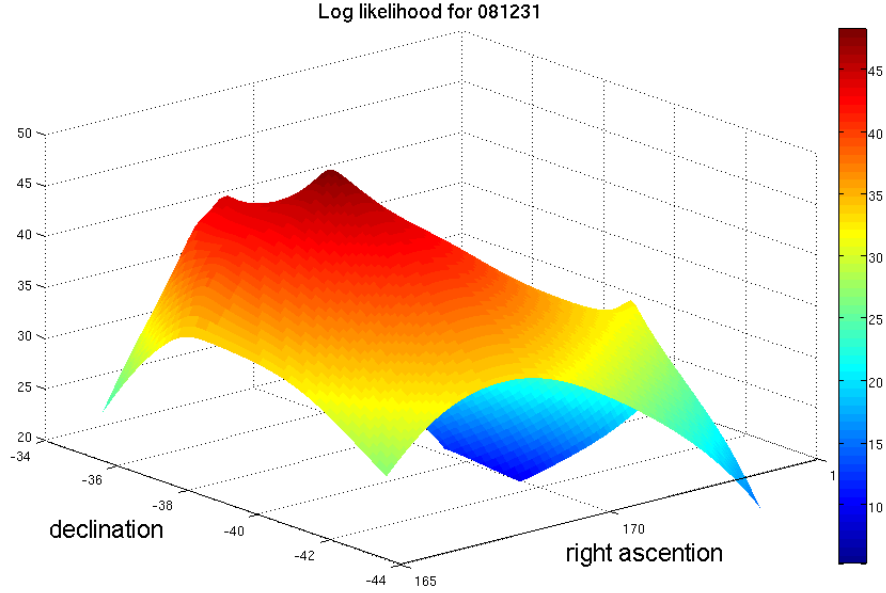


Figure 1. The log of the likelihood function (Eq. 2) for GRB 081231

A change of the spectral index between -1 to -3, yields a change in the calculated position of less than 0.1° . In addition, we verify in §4 that the assumption $N \propto E^{-2}$ results in good agreement with the positions found by the LAT team for LAT detected bursts in the sample. Table 1 describes the positions of the bursts and compares them to the GBM positions. Note that the GBM positions have error bars of 10° and that the most probable position that we calculate may be dominated by the noise. The errors in our locations are calculated according to the decline of the log-likelihood function (Press et al. 1992) and correspond to 68% confidence levels.

3.2 Upper limits for the GBM sample

To obtain upper limits on (or estimate) the GeV fluence we insert a burst-like signal with a known fluence and a given position into the actual data of the burst and mimic the process of identifying the burst's position using the maximum likelihood method (described in §3.1). If the new maximum is closer to the position of the planted signal than to the position found in the original data, the signal is considered to be identified. We repeat this process many times, each time drawing a different realization of the signal from a given distribution. The minimal fluence that the artificial signal must have in order to be identified over the actual burst signal (or background noise) by our method in more than 90% of the realizations is considered as an upper limit to the burst's fluence at a confidence of 90%.

| Burst | Most probable LAT right ascension | Most probable LAT declination | error in location (deg) | GBM right ascension | GBM declination |
|---------|--------------------------------------|----------------------------------|----------------------------|------------------------|--------------------|
| 080906B | 184.3 | -2.3 | 0.4 | 185.5 | -8.6 |
| 080925 | 97.8 | 18.1 | 0.9 | 96.1 | 18.2 |
| 081009 | 251.9 | 17.8 | 1.5 | 251.1 | 17.1 |
| 081207 | 132.1 | 63.6 | 3.7 | 119.2 | 66.9 |
| 081222 | 23.9 | -34.2 | 1.8 | 22.7 | -34.1 |
| 081231 | 218 | -38.1 | 1 | 218 | -38.7 |
| 090117C | 23.8 | -36.5 | 2.6 | 22.8 | -34.1 |
| 090131 | 349.1 | 15.1 | 1.6 | 353 | 16.4 |
| 090330 | 160.8 | -6 | 0.5 | 159.2 | -7.7 |
| 090516A | 139.6 | -15.2 | 0.6 | 138.3 | -11.9 |
| 090516B | 122.5 | -67.9 | 0.3 | 122.2 | -71.6 |
| 090524 | 333.6 | -63.3 | 2.3 | 329.5 | -67.4 |
| 090528B | 312.3 | 35.9 | 2.8 | 312.2 | 32.7 |
| 090711 | 141.8 | -59.4 | 0.3 | 139.6 | -64.7 |
| 090720 | 217.4 | -60 | 1.9 | 203 | -54.8 |
| 090829A | 330.3 | -33.8 | 0.2 | 329.2 | -34.2 |
| 090922A | 13 | 72.1 | 0.45 | 17.1 | 74.3 |
| 091120 | 225.7 | -24.8 | 0.6 | 224.8 | -24.8 |

Table 1. Positions of our “GBM sample” - 18 brightest GBM bursts in the LAT field of view that were not detected by the LAT. The method we use to calculate the most probable LAT position is described in the text

We simulate a source-like signal, assuming a spectrum⁵ $N \propto E^{-2}$. Given the spectrum, the fluence corresponds to an average number of photons, N_{avg} , that composes the simulated signal. We allow for random Poisson fluctuations of $\sqrt{N_{avg}}$ in the number of photons and choose the energy of each photon randomly with a probability defined by the spectrum. The right ascension and declination of each photon are taken according to the PSF and the angle to the detector is determined by the average incidence angle of the actual incoming photons in the relevant time interval at that position. The average bore-sight is taken by considering all the photons arriving after $t=0$ and averaging over their effective areas. The alternative, to give each photon a distinct bore-sight angle, would have required us to make further assumptions regarding the temporal profile of the signal, thus further complicating the analysis. Notice, that even for the maximal slewing during a burst in the sample, which is about 50° , the difference between the actual effective area and the average we use is less than a factor of two. Hence, this is also the maximal error due to slewing in our estimated flux. The consistency of our treatment of slewing is confirmed by the fact that we reproduce the results for LAT bursts with published fluence (see §4).

We center the simulated signal at a random point between 5° to 10° away from the position determined from the original data. This ensures that there is no confusion with the data of the most probable source.

⁵ We have checked in §3.1 that the dependence of bursts’ positions on the spectrum are weak. In addition we verify here that also the upper limits are not highly dependent on the spectrum. As we raise the spectral slope, the signal consists of less energetic photons. This makes the signal harder to detect and therefore raises the limits we obtain. Changing the spectrum from $N \propto E^{-1}$ to $N \propto E^{-3}$ yields an average increase of 25% in the upper limits for 600 sec. In addition the various bursts in the sample have very little spread around this average.

| Burst | 90% upper limit at T_{90} (erg/cm ²) | LAT/GBM fluence upper limit at T_{90} ¹ | Band extrapolated fluence at T_{90} (erg/cm ²) | 90% upper limit at 600 sec (erg/cm ²) | LAT/GBM fluence upper limit at 600 sec |
|---------|--|--|--|---|--|
| 080906B | 9.27×10^{-7} | 0.09 | 8.44×10^{-6} | 4.51×10^{-6} | 0.41 |
| 080925 | 2.03×10^{-6} | 0.15 | 2.24×10^{-6} | 2.03×10^{-6} | 0.69 |
| 081009 | 2.12×10^{-6} | 0.26 | 1.16×10^{-13} | 1.03×10^{-5} | 1.24 |
| 081207 | 2.83×10^{-6} | 0.03 | 1.61×10^{-5} | 8.09×10^{-6} | 0.08 |
| 081222 | 2.47×10^{-6} | 0.18 | 9.69×10^{-6} | 5.1×10^{-6} | 0.38 |
| 081231 | 7.6×10^{-7} | 0.06 | 1.58×10^{-5} | 8.02×10^{-6} | 0.67 |
| 090117C | 1.27×10^{-6} | 0.12 | 8.91×10^{-6} | 5.74×10^{-6} | 0.52 |
| 090131 | 2.07×10^{-6} | 0.1 | 2.67×10^{-6} | 7.9×10^{-6} | 0.35 |
| 090330 | 1.09×10^{-6} | 0.1 | 1.03×10^{-7} | 5.71×10^{-6} | 0.5 |
| 090516A | 4.28×10^{-6} | 0.19 | 8.26×10^{-6} | 4.77×10^{-6} | 0.21 |
| 090516B | 5.31×10^{-6} | 0.18 | N/A ² | 8.57×10^{-6} | 0.29 |
| 090524 | 2.54×10^{-6} | 0.13 | 1.82×10^{-6} | 7×10^{-6} | 0.38 |
| 090528B | 4.1×10^{-6} | 0.09 | 6.06×10^{-6} | 1.24×10^{-5} | 0.27 |
| 090711 | 1.7×10^{-6} | 0.15 | N/A | 1.7×10^{-6} | 0.15 |
| 090720 | 3.63×10^{-6} | 0.34 | 1.71×10^{-6} | 1.28×10^{-5} | 1.2 |
| 090829A | 2.67×10^{-6} | 0.03 | 6.5×10^{-5} | 4.1×10^{-6} | 0.04 |
| 090922A | 3.23×10^{-6} | 0.28 | 1.73×10^{-6} | 1.04×10^{-5} | 0.91 |
| 091120 | 2.46×10^{-6} | 0.08 | 1.51×10^{-8} | 8.4×10^{-6} | 0.28 |

Table 2. Upper limits at 90% confidence level on the GeV fluence of the bursts in the GBM sample, the LAT/GBM fluence ratio and LAT fluence assuming an extrapolation of the GBM Band spectrum. The GBM fluence and spectrum used for extrapolation is taken from Zhang et al., 2010

¹The GBM Fluence was taken in the range of 8-1000keV

²Band parameters are not available

We plant the photons of the simulated signal onto the original data from $t=0$ to $t=T$ (where T is either T_{90} or 600 sec) and again apply the maximum likelihood method. If the new maximum is closer to the position of the planted signal than to the position found in the original data, the signal is considered as detected. We repeat this process a 1000 times for different fluxes and we note the value of $S_{90\%}$ for which the detection probability of the inserted signal reaches 90% .

4 LAT DETECTED BURSTS

As a test for the overall method we apply it to the sample of 10 LAT detected bursts. First, we compare the positions of the LAT bursts we find using the maximum likelihood method, to those reported by the LAT team. A good agreement (a deviation of about 0.5°) is found within the errors of the method with most of the positions reported by the LAT team (see Table 3). Notice that 080825C has a large bore-sight angle ($\theta = 60^\circ$), resulting in a large fraction of photons with extremely small effective areas. This leads to fewer photons (relative to bursts with small bore-sight angles and with a similar flux) and at the same time to an increase in the photon's weighted flux ($E/A(E, \theta)$). The result is a large increase in the statistical error. Indeed the deviation from the LAT position is large in this case (2.1°) but within the estimated error bars. The overall agreement of the positions found with those published by LAT team is an additional confirmation that the

| Burst | calculated ascension | right declination | LAT ascension | right declination | LAT sight (deg) | Bore- angle | difference LAT and locations (deg) | error in location estimate (deg) |
|---------|-------------------------|----------------------|------------------|----------------------|-----------------------|----------------|--|-------------------------------------|
| 080916C | 117.5 | -56.5 | 119.8 | -56.6 | 48 | | 2.3 | 2.5 |
| 080825C | 233 | -2.8 | 233.9 | -4.7 | 60 | | 2.1 | 3.6 |
| 090217 | 205.5 | -8.4 | 204.9 | -8.4 | 34 | | 0.6 | 0.9 |
| 090323 | 190.5 | 17 | 190.7 | 17 | -1 | | 0.2 ¹ | 0.5 |
| 090328 | 91 | -42 | 90.9 | -42 | -1 | | 0.1 ¹ | 0.25 |
| 090626 | 171.1 | -33.3 | 170 | -33.5 | 15 | | 1.1 | 1.5 |
| 090902B | 265.7 | 27.3 | 265 | 27.3 | 52 | | 0.7 | 0.6 |
| 090926A | 353.8 | -66.3 | 353.6 | -66.3 | 52 | | 0.2 | 0.3 |
| 091003A | 253.2 | 36.5 | 251.4 | 36.6 | 13 | | 1.6 | 0.8 |
| 091031 | 71.7 | -57.6 | 71.7 | -57.5 | 22 | | 0.1 | 0.2 |

Table 3. Positions of LAT-detected GRBs found by our calculation compared to those reported by the LAT team (Tajima et al. 2008, Bouvier et al. 2008, Ohno et al. 2009a, Ohno et al. 2009b, McEnery et al. 2009a, Piron et al. 2009, de Palma et al. 2009a, Uehara et al. 2009, McEnery et al. 2009b, de Palma et al. 2009b)

¹No bore-sight angle available

uncertainty in the assumed spectrum of the source isn't crucial in determining the positions, and the results based on the assumption $N \propto E^{-2}$ are valid.

We obtain upper limits and fluence estimates for all LAT bursts. We use the “planted signal” method for the upper limits at a confidence level of 50% instead of 90%. A signal that in 50% of the cases is detected over the original signal must be comparable to the main peak in the data. If one assumes that this peak originates from the burst itself rather than from the noise, the fluence of such a signal should be an estimate to the original burst's fluence. Again 080825C is an exception.

To date, the LAT team published fluence measurements to only four of these bursts (Abdo et al. 2010). We compare the upper limits and fluence estimates to these bursts in Table 4. Our upper limits are consistent with the fluence estimates and with the LAT results. It is noticeable that our estimated fluences tend to overestimate the LAT reported fluence by a factor of ~ 3 . This is possibly due to extra noise cuts applied by the LAT team using a careful treatment of each photon separately. When considering only upper limits to individual bursts this doesn't cause a problem as it simply makes the upper limits more conservative. We also compare our fluence estimates to those of Ghisellini et al. (2010) and find comparable values (figure 6). Note that Ghisellini et al. (2010) also overestimate the fluences reported by the LAT team by a factor of 2-4.

Figs. 2 & 3 depict comparisons of the LAT/GBM fluence ratios of LAT bursts with the upper limits on the LAT/GBM fluence ratio of LAT non-detected bursts for $T = T_{90}$ and $T=600$ sec. The average LAT/GBM fluence ratio for LAT detected bursts is 0.09 (0.2) for T_{90} ($T=600$ sec). These limits are somewhat lower than the corresponding upper limits on these ratios derived for the GBM bursts.

| Burst | 90% Upper limit (erg/cm ²) | 50% detection estimate (erg/cm ²) | Fluence reported by the LAT team (erg/cm ²) |
|---------|---|--|--|
| 080916C | 1.2×10^{-4} | 9.5×10^{-5} | 3.2×10^{-5} |
| 080825C | 7.3×10^{-6} | 4.4×10^{-6} | 3×10^{-6} |
| 090217 | 9.2×10^{-6} | 6.1×10^{-6} | 1.2×10^{-6} |
| 090902B | 1.4×10^{-4} | 1×10^{-4} | 3.9×10^{-5} |

Table 4. A comparison of the 600 sec fluences and upper limits that we calculate for LAT detected bursts, to those reported by the LAT team. The LAT reports are for the total burst fluence (not limited by time after the trigger), but these are dominated by the fluence during the first 600 sec.

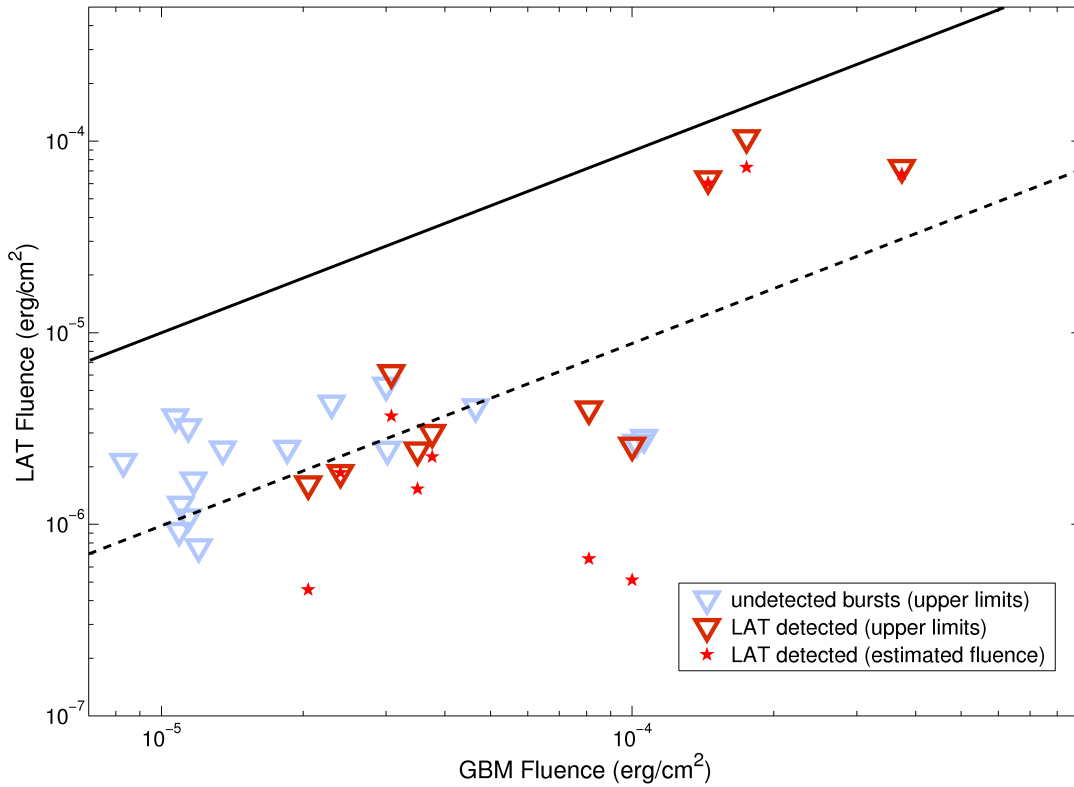


Figure 2. The LAT fluence vs. the GBM fluence for two types of bursts: LAT undetected (the GBM sample) and LAT detected (the LAT sample) bursts, at T_{90} duration. For the GBM bursts we provide upper limits at a 90% confidence level, while for LAT bursts we provide both our upper limits and estimates of the fluence. The solid line marks equal fluence in the LAT and GBM bands, and the dotted line marks a LAT/GBM fluence ratio of 0.1.

5 RESULTS

The results for the duration of T_{90} are summarized in table 2. For the GBM bursts we find upper limits with an average fluence of $S_{90\%}(T_{90}) = 2.4 \times 10^{-6}$ erg/cm², corresponding to an average upper limit of 0.13 on the LAT/GBM fluence ratio. Notice (Fig. 2) that these limits are almost uniform for all GBM bursts and do not seem to depend on the GBM fluence of the bursts. This means that the upper limits derived here are mainly representative of the LAT detection limit (with our method) and do not show any evidence for actual GeV signals in the GBM sample. The upper limits at 600 sec has an average fluence of $S_{90\%}(600s) = 7.3 \times 10^{-6}$ erg/cm², corresponding

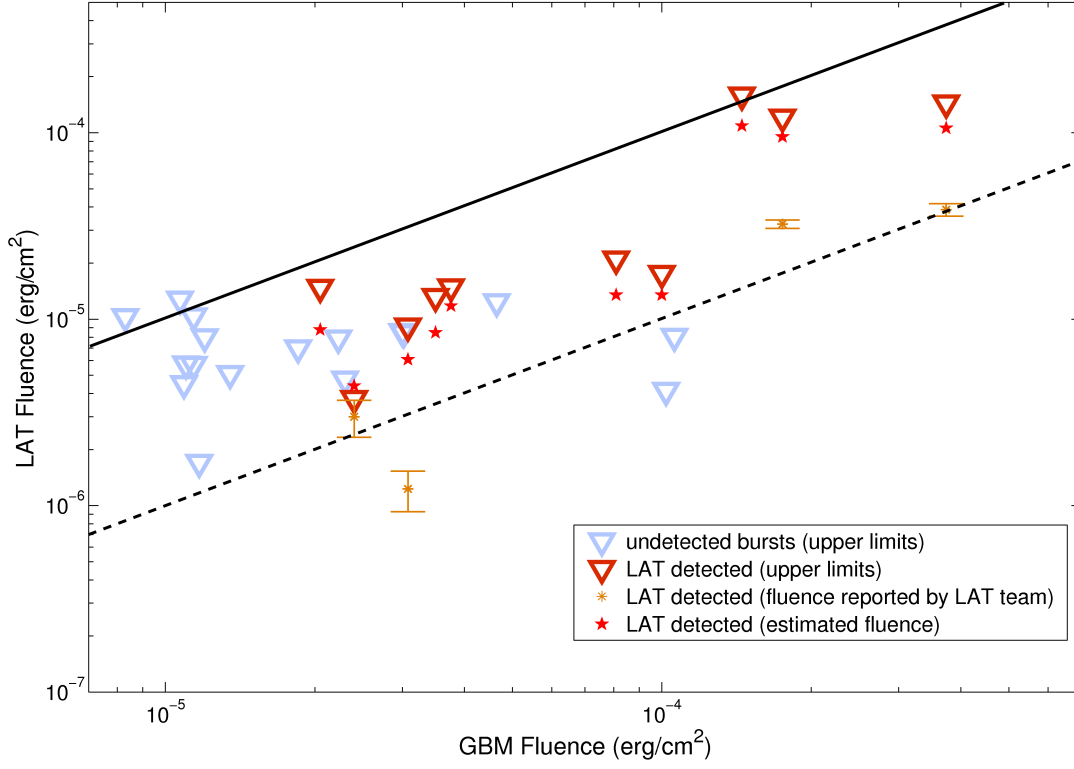


Figure 3. The LAT fluence vs. the GBM fluence for two types of bursts: LAT undetected (the GBM sample) and LAT detected (the LAT sample) bursts, during the first 600 sec after the trigger. For the GBM bursts we provide upper limits at a 90% confidence level, while for LAT bursts we provide both upper limits and actual estimates of the fluence. Also depicted are 4 fluence estimates reported by the LAT team. The solid line marks equal fluence in the LAT and GBM bands, and the dotted line marks a LAT/GBM fluence ratio of 0.1.

to an upper limit of 0.45 on the LAT/GBM fluence ratio. As for the case of T_{90} , Fig. 3 shows almost uniform limits for different GBM fluences. Therefore these limits too, correspond to the LAT detection limit within our method. The fact that the limits here are higher than the T_{90} limits is merely an artifact of the longer timescales and therefore higher noise level. These results are summarized in table 2.

The overall number of bursts detected by LAT is consistent with an extrapolation of the Band function fitted at the MeV range (Le & Dermer 2009) to the GeV range. It is interesting to check whether this extrapolation is consistent with the upper limits we obtain in §3.2. For all bursts in the sample, we take the Band parameters (and corresponding errors) (Band 1993): E_{peak} (the peak in νF_ν), α (the lower energy spectral slope), β (the higher energy spectral slope) as reported in the GCNs. In addition we also take the bursts' T_{90} and the overall fluence in the GBM band. We extrapolate the MeV emission of GBM bursts using the Band function to the LAT energy range [100 MeV - 30 GeV]. We calculate the overall LAT fluence expected for each burst in the sample assuming no break in the spectral index between the GBM and the LAT windows. As we do not

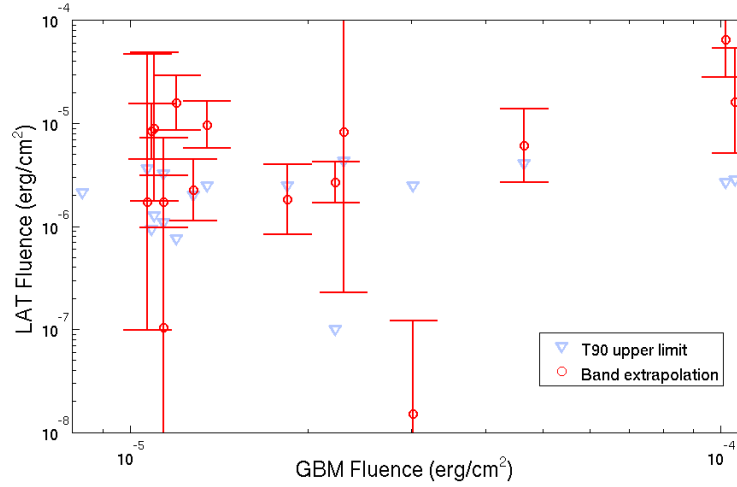


Figure 4. The 100MeV - 10GeV fluence obtained by extrapolation of the GBM Band spectrum to GeV for the GBM sample, compared with the LAT upper limits on the GeV fluence. For two thirds of the sample, the extrapolation of the Band function is consistent with the upper limits. The extrapolated fluence of the remaining five bursts is significantly larger than their upper limits. These bursts suggest a decline in the spectral slope between the MeV and the GeV. 090516B and 090711 have no Band parameters reported in the GCNs (GCN data: Bissaldi et al. 2008a, Goldstein et al. 2008a, von Kienlin et al. 2008, Briggs et al. 2008, Bissaldi et al. 2008b, Goldstein et al. 2008b, Connaughton et al. 2009, Goldstein et al. 2009, von Kienlin et al. 2009a, McBreen et al. 2009a, McBreen et al. 2009b, von Kienlin et al. 2009b, von Kienlin et al. 2009c, Rau et al. 2009a, Wilson et al. 2009, Rau et al. 2009b, Gruber et al. 2009)

have the covariance matrices of the spectral fits, and we don't know the degree of correlation between the various errors, we assume the "worst case scenario". This is to say we take those correlations that maximize the overall error in the fluence estimate. Specifically, this means that when looking for a lower limit on the extrapolation we take the lower values of N_0 and E_p and the higher value of β . Clearly, changing α is also not relevant for the sake of these limits. This is what we refer to as 1σ , it is an overestimate of the actual value. As can be seen in table 2 and in Fig. 4 most expected fluences (9 out of 16) are compatible with the upper limits. In two bursts (e.g. 081009, 091120) the Band extrapolations are a few orders of magnitudes below the upper limits. This is not necessarily significant as these are only upper limits and the actual LAT fluence is unknown and can be low. The rest (5 out of 16), almost a third of the bursts, have Band extrapolations significantly above the upper limits on their T_{90} fluence. In most of these bursts the Band extrapolation is $2-3\sigma$ above our LAT 90% upper limit. Therefore, there is no single burst in which this excess is measured without doubt. However the fact that such a non-negligible excess is observed in a large fraction of the sample is notable, and it suggests an evidence for a decline in the slope of the spectrum at high energies of some bursts.

A similar pattern is observed when we extrapolate MeV emission using the Band function reported by Zhang et al. (2010) for the LAT detected bursts. The comparison of the Band extrapolated fluence and our estimates of the actual T_{90} LAT fluence is depicted in Fig. 5, where we also

present Band extrapolations based on fits reported in GCNs, that in almost all cases⁶ agree with those of Zhang et al. (2010). For the majority of the bursts (080916C, 090217, 090626, 090926A, 091003A, 091031) the Band extrapolated fluence is of order of the LAT estimated fluence. These bursts are consistent with a single spectral component ranging from MeV to GeV (Zhang et al. 2010). In GRB 090902B, the extrapolated fluence is three orders of magnitude lower than its estimated fluence, indicating on an additional source of high energy emission (Abdo et al. 2009b). In the last three bursts (080825C, 090323, 090328) the extrapolated fluence to the GeV range is about an order of magnitude higher ($\sim 3\sigma$) than the estimated GeV fluence. These cases provide again, evidence for a steepening of the high energy spectral slope between the MeV and the GeV bands. Note that GRB 080825C has a large bore-sight angle and therefore our estimates are less reliable for this burst. However, the Band extrapolation for this burst is also above the fluence reported by the LAT team for the entire LAT fluence (not only confined to T_{90}) from this GRB.

Even though the break in the spectrum is not confirmed for any of the bursts individually, we can attempt to estimate the Lorentz factors for those GRBs where we can see a possible steepening in the high energy spectral slope. This is done by assuming that the steepening originates from the increase in the optical depth with photon energy until it reaches order unity at the energy where a break is seen in the spectrum (Lithwick & Sari 2001; Abdo et al. 2009a). We assume that the energy of the break is of the order of 1GeV for these bursts (an increase by a factor of 10 in the break energy, will only change the estimate by a factor ~ 1.5). This yields estimated Lorentz factors of: $\Gamma = 170$ for 090323 and $\Gamma = 190$ for 090328. GRB 080825C has no known redshift, and therefore we can not directly estimate its Lorentz factor. For a generic $z=1$ we obtain $\Gamma = 220$. These results are within the “generic range” expected for the Lorentz factor in GRBs.

The results rule out any model in which there is a strong GeV component in the prompt mission. In particular they limit strongly SSC models for the prompt emission as those will suggest a second SSC component at the GeV (Ando et al. 2008, Piran et al. 2009). They pose a strong limit on the conditions within the emitting regions showing no IC GeV Peak.

⁶ The two sets of results are generally similar except for the case of GRB 090626 where the calculation according to the GCN parameters yields a fluence two orders of magnitude lower than that obtained with the Zhang et al. (2010) parameters. Notice that for GRB 090323 there are no Band parameters in the GCNs.

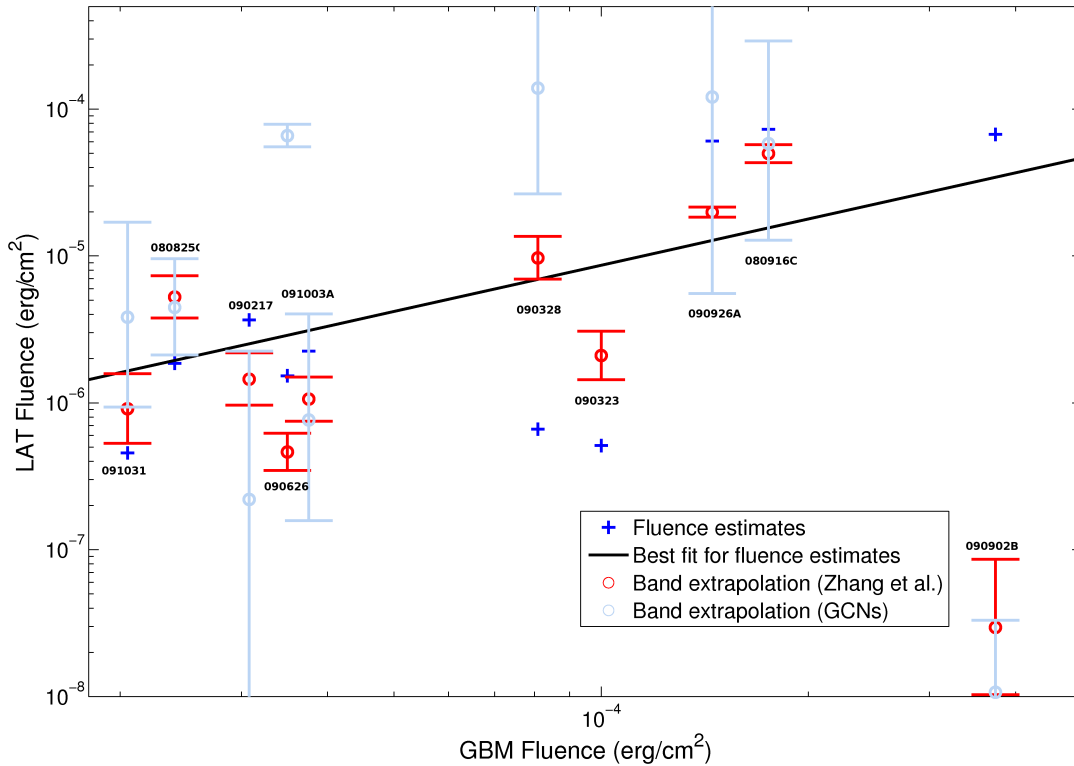


Figure 5. LAT detected bursts at T_{90} . Shown are the fluence estimates and the Band function extrapolations to the GeV range (using Band parameters either from Zhang et al. 2010 or from the GCNs). The solid line marks the best fit for the fluence estimates, its slope is close to 1. This figure shows a positive correlation between LAT and GBM fluence of LAT bursts. GRB 090902B has a low extrapolated fluence of $\sim 10^{-8}$ which falls below the figure. GRB 090323 has no reported Band parameters in the GCNs. Three bursts, whose Band extrapolations are larger than the observed LAT fluences, show evidence for a break in the high energy spectral slope (GCN parameters: van der Horst et al. 2008a, van der Horst et al. 2008b, von Kienlin et al. 2009d, Rau et al. 2009c, von Kienlin et al. 2009e, Bissaldi et al. 2009a, Bissaldi et al. 2009b, Rau et al. 2009d, Golenetskii(2009)).

6 CONCLUSIONS

GeV emission from GRBs is as of yet relatively unexplored observationally. Up to February 2010, only 10 bursts were detected by LAT in the GeV range. Already in this early observational stage, though, there is much information that can be extracted by detailed analysis. This, in turn, provides us with independent tests to the various emitting mechanisms.

We have analyze the group of bursts expected to have the highest (undetected) GeV component. Those are the 18 most luminous GBM bursts with no LAT detection. For these bursts, we obtain upper limits on the GeV fluence. For the whole sample we obtain an average upper limit to the fluence ratio of 0.13 during the prompt phase (T_{90}) and an average upper limit to the ratio of 0.45 for 600 sec. These ratios strongly constrain various emission models and in particular rule out SSC models for either the MeV emission or the GeV component in the prompt emission. In both cases, a significant LAT component is expected.

The fluence estimates for LAT bursts, lead to somewhat lower ratios for the LAT/GBM fluence

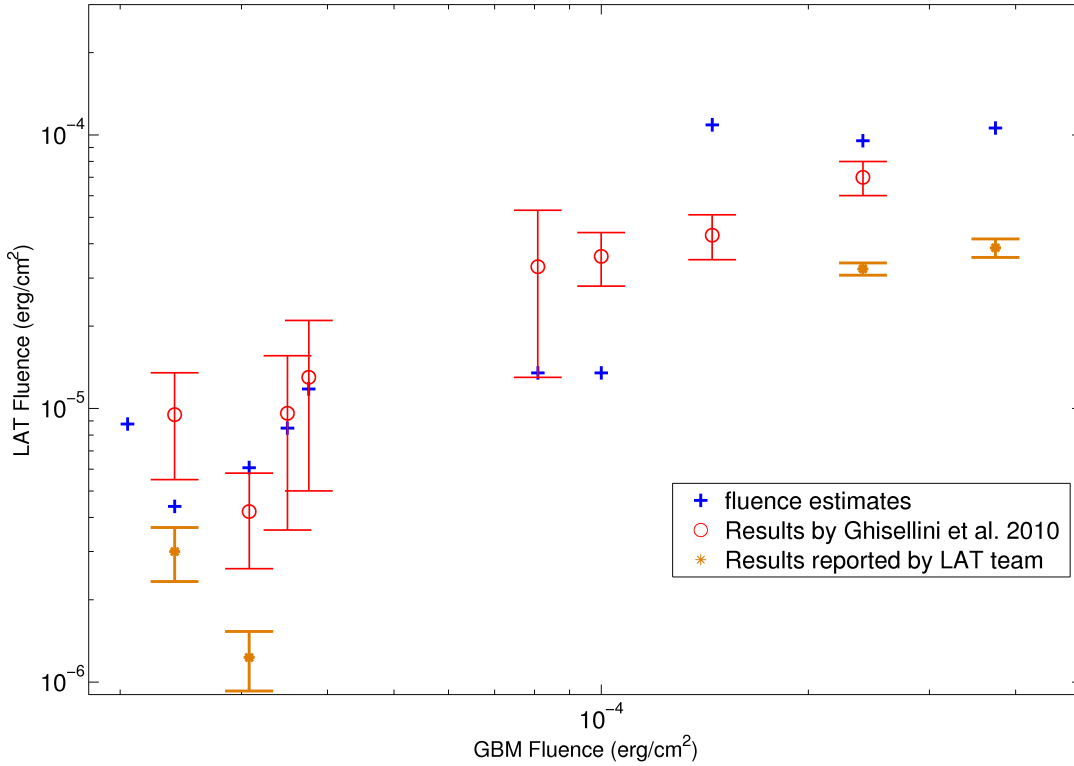


Figure 6. LAT detected bursts at 600 sec: Shown are the fluence estimates. These are compared to results by Ghisellini et al. 2010 and to results reported by the LAT team.

ratio. These are 0.09 ± 0.03 and 0.2 ± 0.09 for the durations of T_{90} and 600 sec respectively (Figs. 5 & 6). In addition, the LAT bursts show a correlation between their LAT and GBM fluences, namely - the stronger a burst is in the GBM band, the stronger it is in the LAT band. Considering that for the LAT undetected bursts there are only upper limits, These results are consistent with the LAT-GBM fluence correlation which is seen in the LAT-detected bursts. Namely, the LAT bursts don't have to be drawn from a different population than the GBM bursts.

For the majority of the GBM and the LAT bursts the GeV fluence is compatible with the Band extrapolation of the MeV emission. However, out of the LAT bursts, in three cases the Band extrapolation of the MeV emission is higher than the observed fluence. Similarly the Band extrapolation is higher than the LAT upper limits in 5 out of 16 GBM bursts. Both results are consistent and suggest that in some bursts we observe a decline in the spectral high energy slope between the MeV and the GeV. This may be the first indication for the long sought after pair opacity break in the high energy spectrum. If so it can enable us to estimate corresponding values of the bulk Lorentz factors which are around a few hundred.

This research was supported by an ERC advanced research grant, by the Israeli center for

Excellent for High Energy AstroPhysics, by the Israel Science Foundation (grant No. 174/08) and by an IRG grant.

REFERENCES

- Abdo A. A., et al., 2009a, *Science*, 323, 1688
- Abdo A. A., et al., 2009b, *ApJ*, 706, L138
- Abdo, A., et al., 2010, *ApJ*, 712, 558
- Ackermann M., et al., 2010, *ApJ*, 716, 1178
- Ando, S., Nakar, E. & Sari, R. 2008, *ApJ* 689, 1150.
- Aoi J., et al., 2009, arXiv:0904.4878v1
- Atwood, W. B., 2009 *ApJ* 697.1071A.
- Band, D., et al. 1993, *ApJ*, 413, 281.
- D. L. Band et al., 2009 *ApJ* 701 1673.
- Bissaldi, E. 2008, GCN circ.,8214.
- Bissaldi, E. 2008, GCN circ.,8715.
- Bissaldi, E. 2009, GCN circ.,9866.
- Bissaldi, E. 2009, GCN circ.,9933.
- Bouvier, A. 2008, GCN circ.,8183.
- Briggs, M. S.2008, GCN circ.,8665.
- Briggs M.S., Connaughton V., Meegan C.A. et al. (2009). *AIP Conf. Proc.* 1133,p. 40.
- Chiang, J., & Dermer C. D. 1999, *ApJ*, 512, 699
- Connaughton, V. 2009, GCN circ.,8822.
- Corsi, A., Guetta, D., Piro, L. 2010, *A&A*, 524, 92.
- de Palma, F. 2009, GCN circ., 9867.
- de Palma, F. 2009, GCN circ., 10163.
- Dermer, C. D. 2008, *ApJ.*, 684, 430
- Finke, J. D., Dermer, C. D., Bottcher, M. 2008, *ApJ*, 686, 181.
- Fan, Y.-Z., & Piran, T. 2008, *Frontiers of Physics in China*, 3, 306.
- Fan, Y.-Z., Piran, T., Narayan, R., & Wei, D.-M. 2008, *MNRAS*, 384, 1483.
- Fan, Y.-Z. 2009, *MNRAS*, 397, 1539.
- Gao W. H., Mao J. R., Xu D., & Fan Y. Z., 2009, *ApJ*, 706, L33
- GBM lookup table - <http://heasarc.gsfc.nasa.gov/W3Browse/fermi/fermigbrst.html>

- Ghisellini G., Ghirlanda G., Nava L. & Celotti A., 2010, MNRAS, 403, 926
- Gonzalez, M. M., Dingus, B. L., Kaneko, Y., Preece, R. D., Dermer, C. D., and Briggs, M. S. 2003, Nature, 424, 749.
- Goldstein, A. 2008, GCN circ., 8291.
- Goldstein, A. 2008, GCN circ., 8781.
- Goldstein, A. 2009, GCN circ., 8876.
- Golenetskii, S. 2009, GCN circ., 10166.
- Gonzalez Sanchez M. M., 2005, Ph.D. Thesis.
- Granot, J., & Guetta, D. 2003, ApJ 598L, 11.
- Gruber, D. 2009, GCN circ., 10187.
- Guetta, D., & Granot, J. 2003, ApJ, 585, 885.
- Guetta, D., Pian, E., Waxman, E. 2011, A&A, 525, 53.
- Hurley, K. et al. 1994, Nature, 372, 652.
- Klebesadel, R.W., Strong, I.B., & Olson, R.A. 1973, ApJ, Lett., 182, L85.
- Kumar P., & Barniol Duran R., 2009, MNRAS, 400, L75
- Kumar P., & Barniol Duran R., 2010, arXiv:0910.5726
- Kumar, P. & McMahon, E. 2008, MNRAS, 384, 33.
- LAT lookup table - <http://fermi.gsfc.nasa.gov/ssc/observations/types/grbs>
- Lithwick, Y., & Sari, R. 2001, ApJ, 555, 540
- Le T., & Dermer C. D., 2009, ApJ, 700, 1026.
- McBreen, S. 2009, GCN circ., 9415.
- McBreen, S. 2009, GCN circ., 9413.
- McEnery, J. 2009, GCN circ., 9044.
- McEnery, J. 2009, GCN circ., 9985.
- Meegan, C., et al. 2009, ApJ, 702, 791.
- Mészáros, P., Rees, M. J., & Papathanassiou, H. 1994, ApJ, 432, 181.
- Nakar, E., Ando, S., & Sari, R. 2009, Apj, 703, 675.
- Ohno, M. 2009, GCN circ., 8903.
- Ohno, M. 2009, GCN circ., 9021.
- Panaitescu, A., & Mészáros, P. 2000, ApJ, 544, L17.
- Panaitescu, A., & Kumar, P. 2000, ApJ, 543, 66.
- Piran T., & Nakar E., 2010, ApJ, 718, L63.
- Piran, T., Sari, R., & Zou, Y. 2009, MNRAS, 393, 1107.

- Piron, F. 2009, GCN circ., 9584.
- Press, W. H., Teukolsky, S. A., Vetterling, W. T., & Flannery, B. P. 1992, Numerical recipes in FORTRAN. The art of scientific computing (Cambridge: University Press, —c1992, 2nd ed.)
- Rau, A. 2009, GCN circ., 9688.
- Rau, A. 2009, GCN circ., 9929.
- Rau, A. 2009, GCN circ., 9057.
- Rau, A. 2009, GCN circ., 9983.
- Sari, R., Narayan, R., & Piran, T. 1996, ApJ, 473, 204.
- Sari, R., & Esin, A. A. 2001, ApJ, 548, 787.
- Schneid, E.J., et al. 1992, A&A, 255, L13.
- Schneid E. J., Bertsch D. L., Dingus B. L. et al. 1995, ApJ, 453, 95.
- Swenson C. A., et al., 2010, ApJ, 718, L14.
- Tajima H. 2008, GCN circ., 8246.
- Uehara, T. 2009, GCN circ., 9934.
- van der Horst, A. J. 2008, GCN circ., 8278.
- van der Horst, A. J. 2008, GCN circ., 8184.
- von Kienlin, A. 2008, GCN circ., 8374.
- von Kienlin, A. 2009, GCN circ., 9055.
- von Kienlin, A. 2009, GCN circ., 9424.
- von Kienlin, A. 2009, GCN circ., 9447.
- von Kienlin, A. 2009, GCN circ., 8902.
- von Kienlin, A. 2009, GCN circ., 9579.
- Waxman, E. 1997, ApJ, 485, L5.
- Wei, D. M., & Lu, T. 1998, ApJ, 505, 252.
- Wilson, A. C. 2009, GCN circ., 9849.
- Xue R. R., Fan Y. Z., & Wei D. M., 2008, MNRAS, 389, 321.
- Zhang, B., & Mészáros, P. 2001, ApJ, 559, 110.
- Zhang, B. B., et al. 2010, ApJ, arXiv:1009.3338
- Zhao X. H., Li Z., & Bai J. M., 2010, arXiv:1005.5229
- Zou, Y., Fan, Y., Piran, T., arXiv, 1008.2253.